and one that was not, which were identified on the basis of the V_β-J_β profile.
13. E. C. Dudley, H. T. Petrie, L. M. Shah, M. J. Owen, A. Hayday, *Immunity* **1**, 83 (1994); H. von Boehmer and H. J. Fehling, *Annu. Rev. Immunol.* **15**, 433 (1997).
14. C. Benit, B. Lucas, F. Vasseur, *J. Immunol.* **154**, 5103 (1995); H.-M. Rodewald and H. J. Fehling, *Adv. Immunol.* **69**, 1 (1998).
15. A. Casrouge *et al.*, in preparation; L. Gapin *et al.*, *J. Exp. Med.* **187**, 1871 (1998).
16. C. Trigueros *et al.*, *J. Exp. Med.* **188**, 1401 (1998).
17. P. Borgulya, H. Kishi, Y. Uematsu, H. von Boehmer, *Cell* **69**, 529 (1992); C. J. MacMahan and P. J. Fink, *Immunity* **9**, 637 (1998); E. Padovan *et al.*, *Science* **262**, 422 (1993).
18. G. J. V. Nossal, *Cell* **76**, 229 (1994); H. von Boehmer, *ibid.*, p. 219.
19. J. D. Altman *et al.*, *Science* **274**, 94 (1996); D. H. Busch, I. Pilip, E. G. Pamer, *J. Exp. Med.* **188**, 61 (1998); E. A. Butz and M. J. Bevan, *Immunity* **8**, 167 (1998).
20. V. P. Argaet *et al.*, *J. Exp. Med.* **180**, 2335 (1994); P. J. Lehner *et al.*, *ibid.* **181**, 79 (1995); P. A. H. Moss *et al.*, *Proc. Natl. Acad. Sci. U.S.A.* **88**, 8987 (1991).
21. C. Tanchot, F. A. Lemonnier, B. Pérarnau, A. A. Freitas, B. Rocha, *Science* **276**, 2057 (1997); C. Tanchot and B. Rocha, *Immunol. Today* **19**, 575 (1998).
22. S. P. Berzins, R. L. Boyd, J. F. A. P. Miller, *J. Exp. Med.* **187**, 1839 (1998).
23. D. C. Douek *et al.*, *Nature* **396**, 690 (1998).
24. We thank P. Bousso, A. Cumano, A. Vaheri, O. Vapalahti, and M. Viljanen for comments on the manuscript. Supported by the European Molecular Biology Organization and Academy of Finland (T.P.A.) and Ligue Nationale Contre le Cancer.

4 June 1999; accepted 20 September 1999

Arabidopsis NPH3: A NPH1 Photoreceptor–Interacting Protein Essential for Phototropism

Andrei Motchoulski and Emmanuel Liscum*

Phototropism of *Arabidopsis thaliana* seedlings in response to a blue light source is initiated by nonphototropic hypocotyl 1 (NPH1), a light-activated serine-threonine protein kinase. Mutations in three loci [*NPH2*, root phototropism 2 (*RPT2*), and *NPH3*] disrupt early signaling occurring downstream of the NPH1 photoreceptor. The *NPH3* gene, now cloned, encodes a NPH1-interacting protein. NPH3 is a member of a large protein family, apparently specific to higher plants, and may function as an adapter or scaffold protein to bring together the enzymatic components of a NPH1-activated phosphorelay.

Plants are able to sense and respond to changes in light quality, quantity, and direction through the action of a number of photoreceptors and associated signal-response systems. A variety of photoreceptor molecules, such as the red or far-red light–absorbing phytochromes (phy) and blue light–absorbing cryptochromes (cry) (*1*, *2*) have been characterized. Components functioning downstream of such photoreceptors include two photoreceptor-interacting proteins PIF3 and PKS1, which are both phytochrome-interacting proteins (*3*). Potential postperception signaling components identified through mutational analyses (*1*, *2*) include a set of genes in *Arabidopsis* (*NPH2*, *RPT2*, and *NPH3*) that is required for phototropism, or the bending response of plant organs toward or away from directional light stimuli (*4*, *5*).

Null mutations in the *NPH3* locus abolish phototropic responses of etiolated seedlings to blue light at a low fluence rate (*4*) (Fig. 1A). A similar aphototropic phenotype is observed with seedlings carrying null mutations at the *NPH1* locus (*4*) (Fig. 1A), which encodes NPH1, a primary photoreceptor for phototropism (*6*–*8*). However, mutations in neither *NPH1* nor *NPH3* affect other light-dependent responses, such as blue light– and red light–dependent hypocotyl growth inhibition (Fig. 1, B and C). Moreover, despite efforts to identify additional alterations in development, the only clear phenotypic changes observed in *nph1* and *nph3* mutants are those associated with phototropism (*9*). The phototropism-specific phenotypes of the *nph1* and *nph3* mutants imply that NPH1 and NPH3 act in the same genetic pathway and suggest that NPH3 may function biochemically close to the photoperception event mediated by NPH1.

We have cloned the *NPH3* gene by positional cloning (Fig. 2A). Several predicted genes mapping to the region containing the *NPH3* locus (Fig. 2A) were sequenced in mutant backgrounds to identify the *NPH3* gene (Fig. 2B). A full-length *NPH3* cDNA was isolated (*10*) and found to encode a protein of 745 amino acids (*11*) (Fig. 2C). NPH3 is, however, part of a family of proteins in *Arabidopsis* (*12*). Although *NPH3*-related sequences have also been found in other plant species, no paralogous sequences have been found outside the plant kingdom (*9*).

Four regions of sequence conservation have been identified within the NPH3 family (*12*) (Fig. 2C). Region IV exhibits the highest level of sequence identity within the family (≥52.5%, relative to NPH3), with two motifs being most prominent: LYRAID and HAAQNERLPL (*13*) (Fig. 2C). The functional importance of these conserved sequence motifs is currently unknown. However, Tyr^{545} within the LYRAID motif is part of a consensus phosphorylation site ([RK]-x(2,3)-[DE]-x(2,3)-Y; where x(2,3) can be any two or three amino acids) (*14*), in which the Arg, Asp, and Tyr are invariant across the entire NPH3 family (*12*), and deletion of this residue in the *nph3-2* mu-

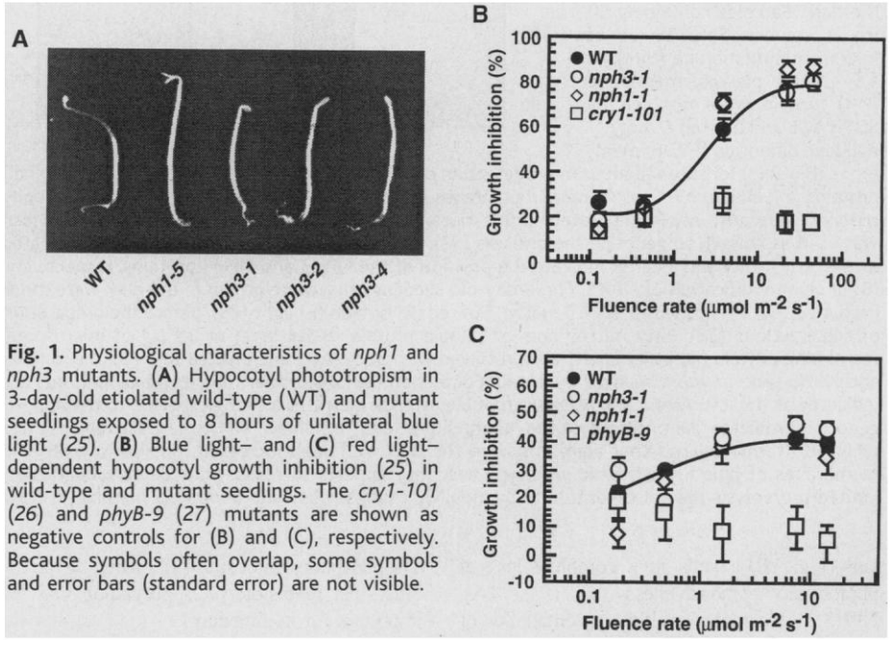

Fig. 1. Physiological characteristics of *nph1* and *nph3* mutants. (**A**) Hypocotyl phototropism in 3-day-old etiolated wild-type (WT) and mutant seedlings exposed to 8 hours of unilateral blue light (*25*). (**B**) Blue light– and (**C**) red light–dependent hypocotyl growth inhibition (*25*) in wild-type and mutant seedlings. The *cry1-101* (*26*) and *phyB-9* (*27*) mutants are shown as negative controls for (B) and (C), respectively. Because symbols often overlap, some symbols and error bars (standard error) are not visible.

Division of Biological Sciences, University of Missouri, Columbia, MO 65211, USA.

*To whom correspondence should be addressed. E-mail: liscumm@missouri.edu

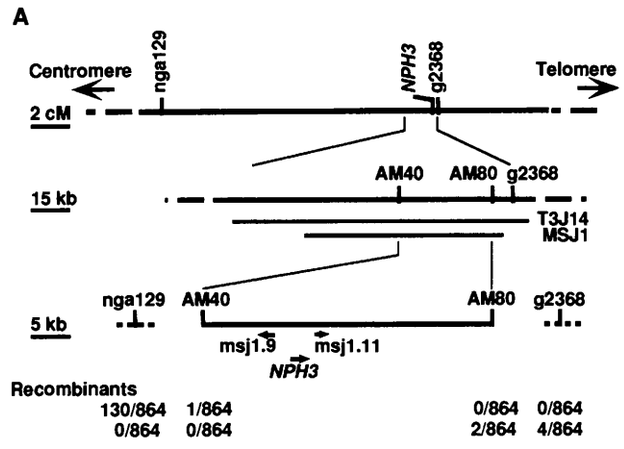

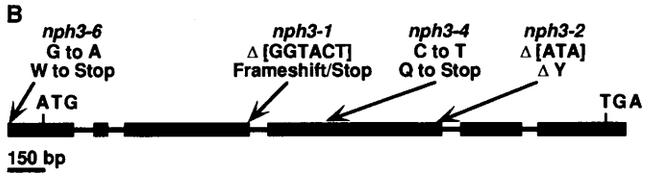

C

```
*nph3-6
MWESESDGGVGVGGGGGREYGDGVLSSNKHGGVKTDGFELRGQSWFVATD  50
IPSDLLVKIGDMNFHLHKYPLLSRSGKMNRLIYESRDPDPTILILDDLPG 100
GPEAFELASKFCYGVPVDLTATNISGLRCAAEYLEMTEDLEEGNLIFKTE 150
AFLSYVVLSSWRDSILVLKSCEKLSPWAENLQIVRRCSESIAWKACSNPK 200
GIRWAYTGKAPSPSTTNFAGSSPRWNESKDSSFYCSPSRNTNSQPVPPDW 250
                    *nph3-1
WFEDVSILRIDHFVRVITAIKVKGMRFELLGAVIMHYAGKWLPGLIKEGG 300
VAIAPAMSSAIGGGLGLGGDEMSISCGSNSSGGSSGPDWKGGLHMVLSAG 350
     *nph3-4
KTNGHQDSVACLAGLGISPKDQRMIVESLISIIPPQKDSVTCSFLLRLLR 400
AANMLKVAPALITELEKRVGMQFEQATLQDLLIPGYNNKGETMYDVDLVQ 450
RLLEHFLVQEQTEGSSPSRMSPSPSQSMYADIPRGNNNNGGGGGGNNQNA 500
                                        *nph3-2
KMRVARLVDSYLTEVARDRNLPLTKFQVLAEALPESARTCDDGLYRAIDS 550
YLKAHPTLSEHERKRLCRVMDCQKLSMDACMHAAQNERLPLRVVVQVLFS 600
EQVKISNALANTSLKESTTLGEAKGTYQPMIPNRKTLIEATPQSFQEGWA 650
AAKKDINTLKFELETVKTKYVELQNEMEVMQRQFEKTGKVKNTPSSSAWT 700
SGWKKLSKLTKMSGQESHDISSGGEQAGVDHPPPRKPRRWRNSIS      745
```

Fig. 2. *NPH3* cloning, gene structure, and amino acid sequence. (**A**) Mapping of *NPH3* on chromosome 5. Initial mapping placed *NPH3* between simple sequence length polymorphism (SSLP) marker nga129 (*28*) and restriction fragment length polymorphism marker g2368 (*29*). Sequence of phagemid P1 clone, MSJ1 (AB008268), was used to generate two new SSLP markers, AM40 and AM80 (*30*), which were used to narrow the potential *NPH3* coding region to three predicted genes: msj1.9, msj1.10, and msj1.11 (*31*). msj1.10 was identified as *NPH3* by sequencing multiple *nph3* mutant alleles (*24*). T3J14 is a BAC clone (*22*). Numbers of recombinants for each marker are shown on the bottom. cM, centimorgan. (**B**) Structure of the *NPH3* gene and positions of *nph3* mutations. The locations of start (ATG) and stop (TGA) codons are indicated. Exon (boxes) and intron (lines) positions were determined by a comparison of the genomic and cDNA sequences. Position and identity of various *nph3* mutations are indicated. (**C**) Deduced amino acid sequence (*13*) of NPH3. Amino acid residues are numbered at the right. Bold-faced residues indicate regions of sequence conserved across the NPH3 family (*12*). Motifs of highest sequence conservation are boxed. The BTB/POZ and coiled-coil domains are underlined with single and double lines, respectively. Locations of *nph3* mutations are indicated by asterisks. In the *nph3-1* allele, amino acids 272 to 295 are replaced with residues (LHIGYFSLKHFHKHLVYISQSSIH) before insertion of a stop codon at position 296.

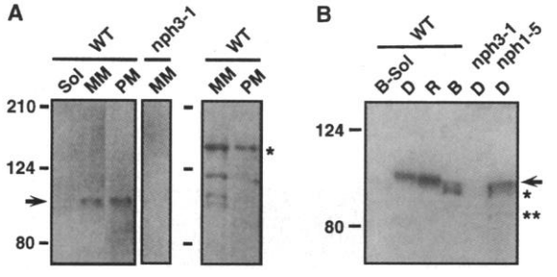

Fig. 3. Plasma membrane localization and in vivo modification of NPH3. (**A**) Immunoblot analysis of NPH3 localization after cell fractionation (*32*) of 3-day-old seedlings that were grown in the dark. Samples containing 50 μg of soluble (Sol), 15 μg of microsomal membrane (MM), or 1.5 μg of plasma membrane (PM) protein were resolved by SDS-PAGE and blotted to polyvinylidene difluoride (PVDF) membrane (Bio-Rad) for subsequent immunodetection of NPH3 (left two panels) and NPH1 (right panel) proteins (*21, 33*). *nph3-1* microsomal membranes represent a negative control for NPH3 antibody specificity, because any NPH3 protein in this mutant lacks the COOH-terminus (see Fig. 2B), which was used as antigen to generate the antisera (*33*). Molecular masses (in kilodaltons) are indicated at the left. Arrow and asterisk indicate the position of the NPH3 and NPH1 proteins, respectively. (**B**) In vivo modification of NPH3. Three-day-old seedlings that were grown in the dark were mock irradiated (D), or exposed to $10^{3.5}$ μmol m^{-2} of red (R) or blue (B) light (*25*), before the preparation of cell fractions (*32*). Fifty micrograms of soluble protein (B-Sol lane) or 15 μg of microsomal membrane protein (all other lanes) were resolved with SDS-PAGE and blotted to PVDF membrane; and NPH3 protein was visualized by immunodetection (*23*). Molecular masses (in kilodaltons) are indicated at the left. Arrow and asterisks (double asterisk indicates a change specific to the *nph1-5* genotype) indicate the positions of the "unmodified" and "modified" NPH3, respectively, relative to NPH3 from seedlings that were grown in the dark. Although increased mobility of NPH3 in membranes of blue light–treated wild-type seedlings appears to result from dephosphorylation, limited proteolysis may also contribute to mobility changes observed in *nph1-5* membranes (*9*).

tant (Fig. 2B) results in a complete loss of phototropic responsiveness (*4*) (Fig. 1A). NPH3 also contains multiple potential Ser or Thr phosphorylation sites (*9*), raising the possibility that reversible phosphorylation may be important for its function.

Primary sequence and secondary structure analyses have also identified two potential protein-protein interaction domains in NPH3. First, a BTB (*broad complex, tramtrack,* and *bric à brac*)/POZ (pox virus and zinc finger) domain (*15, 16*) was found within the NH_2-terminal portion of NPH3 (Fig. 2C), as well as within two additional NPH3 family members (*12*). Second, a coiled coil (*15, 17*) was identified in the COOH-terminus of NPH3 (Fig. 2C), and although sequence divergent, it was also found in a conserved position in eight additional members of the family (*12*). BTB/POZ domains and coiled coils have been found in a large number of proteins with quite disparate functions, and both are capable of mediating self-dimerization and self-multimerization or hetero-dimerization and hetero-multimerization with unrelated domains (*16, 17*).

Although NPH3 is largely hydrophilic and α helical in nature (*18*) and thus anticipated to be soluble, cell fractionation studies indicate that NPH3 is plasmalemma associated (Fig. 3A). Whereas the membrane localization does not change in response to in vivo irradiation, the mobility of NPH3 in SDS–polyacrylamide gel electrophoresis (SDS-PAGE) is enhanced in membrane fractions from seedlings that were irradiated with blue, but not red, light (Fig. 3B).

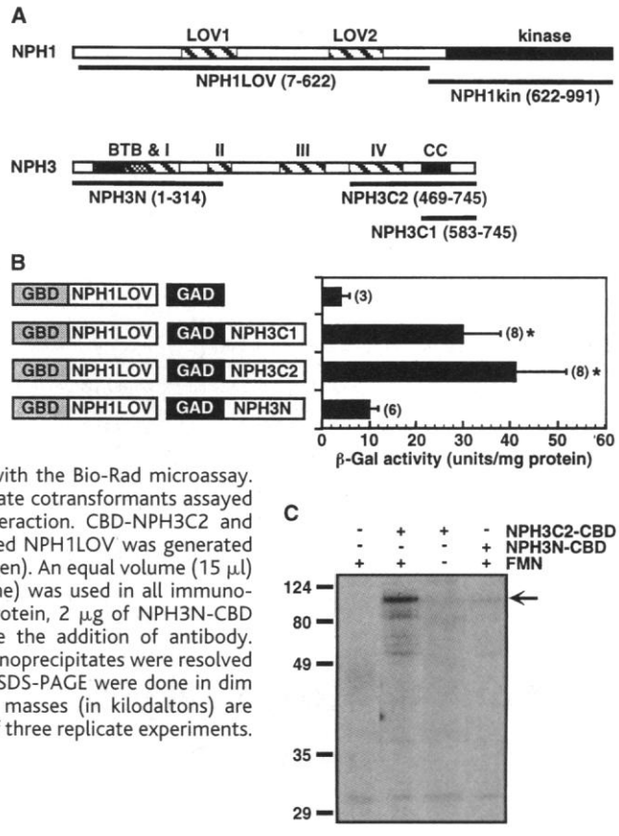

Fig. 4. NPH1-NPH3 interaction. (**A**) Diagrammatic representations of NPH1 and NPH3. The NPH1 protein kinase and LOV domains (*6*) are shown as solid and cross-hatched blocks, respectively. The four conserved sequence domains (I to IV) of the NPH3 family are shown on NPH3 by cross-hatched blocks, and the BTB/POZ and coiled-coil domains are shown as solid blocks. The shaded cross-hatched region of NPH3 indicates where the BTB/POZ domain and domain I overlap. Portions of NPH1 and NPH3 used for interaction studies are indicated below each block diagram. Amino acid residues (positions within full-length proteins) used for each construct are shown in parentheses. (**B**) Yeast two-hybrid assay of NPH1-NPH3 interaction. All combinations of NPH1 and NPH3 polypeptides shown in (A) were initially tested for β-galactosidase (β-Gal) activity by colony filter-lift assay (*34*); however, only NPH1LOV-NPH3C1, NPH1LOV-NPH3C2, and NPH1LOV-NPH3N combinations gave a positive reaction (*9*). Hence, quantitative solution assays of β-Gal activity (*34*) are presented (right) only for those cotransformants. GBD-NPH1 and GAD-NPH3 constructs (*34*) are shown at the left. The GBD-NPH1LOV/GAD cotransformant is shown as a negative control. All yeast growth occurred in darkness. One unit of β-Gal activity is defined as the amount of enzyme that converts 1 nmol of *o*-nitropheynl-β-D-galactopyranoside to *o*-nitrophenol in 1 min at 30°C (pH 7.0); 1 nmol/ml of *o*-nitrophenol has an optical density at 420 nm of 4.5×10^{-3} (*35*). Protein contents of assay solutions were determined with the Bio-Rad microassay. Significant interactions ($0.1 > {}^*P > 0.05$, Students *t* test) and number of replicate cotransformants assayed are indicated; error bars indicate SD. (**C**) In vitro assay of NPH1-NPH3 interaction. CBD-NPH3C2 and CBD-NPH3N fusion proteins were generated as described (*33*). Sulfur-35–labeled NPH1LOV was generated by in vitro transcription and translation with the pT7Blue-2Ek/LIC system (Novagen). An equal volume (15 μl) of ^{35}S-labeled NPH1LOV from the same in vitro translation (60 μl total volume) was used in all immunoprecipitation reactions. Where indicated with a plus, 2 μg of NPH3C2-CBD protein, 2 μg of NPH3N-CBD protein, or 1 μM (final concentration) FMN were added to reactions before the addition of antibody. Polyclonal antibodies against CBD (Novagen) were added to each reaction, immunoprecipitates were resolved with SDS-PAGE, and gels were dried and exposed to x-ray film. All steps up to SDS-PAGE were done in dim red light (*4*). The position of NPH1LOV is indicated by an arrow. Molecular masses (in kilodaltons) are indicated at the left. Although not shown, similar results were obtained in each of three replicate experiments.

A similar enhanced mobility of NPH3 was observed in membranes from *nph1-5* mutant seedlings (Fig. 3B) that were grown in the dark and lack NPH1 (*6*, *7*). One interpretation of these observations is that NPH3 normally interacts with NPH1 in seedlings that were grown in the dark, either directly or indirectly through a protein complex, preventing its modification by other factors, whereas blue light–induced changes in NPH1, such as autophosphorylation (*7*), or simple removal of NPH1, expose sites on NPH3 for modification.

Given the apparent genetic coupling of their protein activities (*4*) (Fig. 1), colocalization to the plasmalemma (*6*, *7*) (Fig. 3A), and potential interaction suggested by in vivo irradiation studies (Fig. 3B), we used a yeast two-hybrid assay (*19*) to directly test whether NPH1 and NPH3 physically interact. Although all combinations of NPH1 and NPH3 fragments shown in Fig. 4A were tested, significant interactions were only observed between coiled-coil–containing NPH3 polypeptide fragments and the NH_2-terminal two-thirds of NPH1 (Fig. 4B), which contains the chromophore-binding LOV (light, oxygen, or voltage) domains (*6*, *7*). Two hybrid results were confirmed by in vitro interaction studies, in which we assayed the ability of a radiolabeled NH_2-terminal NPH1 fragment to be immunoprecipitated by antibodies against a cellulose binding domain (CBD), in the absence or presence of nonlabeled CBD-NPH3 fusion proteins (Fig. 4C). Although CBD antibodies were incapable of precipitating NPH1 itself, a NPH1-containing immunoprecipitate was obtained when coiled-coil–containing NPH3-CBD fusion protein (NPH3C2-CBD) was included in the precipitation reaction (Fig. 4C). The NPH3C2-CBD–dependent immunoprecipitation of NPH1 was not the result of nonspecific interaction with CBD, as a BTB/POZ-containing NPH3-CBD fusion protein did not promote a similar immunoprecipitation response (Fig. 4C). The flavin mononucleotide (FMN)–dependent interaction of NPH1 and NPH3 (Fig. 4C) likely reflects a conformational stabilization of the NPH1 holoprotein in relation to the apoprotein alone, a feature common to many cofactor-containing proteins, including flavin-binding proteins (*20*).

Together, all of the results presented here indicate that NPH3 interacts with the chromophore-binding portion of NPH1, probably through its coiled-coil region, and that this protein complex is necessary for early phototropic signaling. The biochemical function of NPH3, however, remains unknown. In animal and fungal systems, multimolecular signaling complexes using protein kinases and phosphatases are often assembled around a class of proteins known as adapter or scaffold proteins, which contain multiple protein-protein interaction domains (*21*). NPH3 contains at least two protein-protein interaction domains, one of which promotes interaction with NPH1, and early phototropic signaling probably occurs through a NPH1-activated phosphorelay (*2*, *4*). Thus, NPH3 may function as an adapter or scaffold protein in plants. Given their homologies to NPH3, other members of the NPH3 family may also function as adapter or scaffold proteins. Protein complexes assembled by the NPH3 family could provide a means of optimizing speed, specificity, and selectivity of early signaling events associated with a variety of physiological responses, while minimizing undesired cross talk with other response pathways. The identification of such a class of proteins could have broad implications for studies of plant signal transduction.

References and Notes

1. P. H. Quail, *Plant Cell Environ.* **20**, 657 (1998); W. R. Briggs and E. Huala, *Annu. Rev. Cell Dev. Biol.* **15**, 33 (1999).
2. C. Fankhauser and J. Chory, *Curr. Biol.* **9**, 123 (1999).
3. M. Ni, J. M. Tepperman, P. H. Quail, *Cell* **95**, 657 (1998); C. Fankhauser *et al.*, *Science* **284**, 1539 (1999).
4. E. Liscum and W. R. Briggs, *Plant Cell* **7**, 473 (1995); *Plant Physiol.* **112**, 291 (1996).
5. K. Okada and Y. Shimura, in *Arabidopsis*, E. M. Meyerowitz and C. R. Somerville, Eds. (Cold Spring Harbor Laboratory Press, Plainview, NY, 1994), p. 665–684.
6. E. Huala *et al.*, *Science* **278**, 2120 (1997).
7. J. M. Christie *et al.*, *Science* **282**, 1698 (1998); J. M. Christie, M. Salomon, K. Nozue, M. Wada, W. R. Briggs, *Proc. Natl. Acad. Sci. U.S.A.* **96**, 8779 (1999).
8. G. Lasceve *et al.*, *Plant Physiol.* **120**, 605 (1999).
9. A. Motchoulski and E. Liscum, unpublished data.
10. A 6.4-kb Afe I fragment of *NPH3*, isolated from bacterial artificial chromosome (BAC) clone T3J14 (*22*), was used to probe size-selected cDNA libraries [J. J. Kieber, M. Rothenberg, G. Roman, K. A. Feld-

mann, J. R. Ecker, *Cell* **72**, 427 (1993)] (*23*). The largest of 16 independent *NPH3* cDNAs was sequenced (*24*) completely (GenBank accession number AF180390).
11. GenBank searches were accomplished with the gapped BLAST program [S. F. Altschul *et al.*, *Nucleic Acid Res.* **25**, 3389 (1997)].
12. The data are available at www.sciencemag.org/feature/data/1042358.shl.
13. Single-letter abbreviations for the amino acid residues are as follows: A, Ala; C, Cys; D, Asp; E, Glu; F, Phe; G, Gly; H, His; I, Ile; K, Lys; L, Leu; M, Met; N, Asn; P, Pro; Q, Gln; R, Arg; S, Ser; T, Thr; V, Val; W, Trp; and Y, Tyr.
14. T. Patschinsky, T. Hunter, F. S. Esch, J. A. Cooper, B. M. Sefton, *Proc. Natl. Acad. Sci. U.S.A.* **79**, 973 (1982).
15. The BTB/POZ domain was identified with SMART [J. Schultz, F. Milpetz, P. Bork, C. P. Ponting, *Proc. Natl. Acad. Sci. U.S.A.* **95**, 5857 (1998)]. The coiled-coil structure was identified with COILS [A. Lupas, M. Van Dyke, J. Stock, *Science* **252**, 1162 (1991)].
16. O. Albagli, P. Dhordain, C. DeWeindt, G. LeCocq, D. LePince, *Cell Growth Differ.* **6**, 1193 (1995); L. Aravind and E. V. Koonin, *J. Mol. Biol.* **285**, 1353 (1999).
17. C. Cohen and D. A. D. Parry, *Proteins* **7**, 1 (1990); A. Lupas, *Trends Biochem. Sci.* **21**, 375 (1996).
18. Structural analyses were performed with the Protean program (DNASTAR, Madison, WI).
19. S. Fields, *Methods* **5**, 116 (1993); S. Fields and R. Sternglanz, *Trends Genet.* **10**, 286 (1994).
20. M. Nagao and K. Tanaka, *J. Biol. Chem.* **267**, 17925 (1992).
21. M. C. Faux and J. D. Scott, *Cell* **85**, 9 (1996); T. Pawson and J. D. Scott, *Science* **278**, 2075 (1997); E. A. Elion, *Science* **281**, 1625 (1998).
22. S. D. Choi, R. Creelman, J. Mullet, R. A. Wing, *Weeds World* **2**, 17 (1995), http://genome-www.stanford.edu/Arabidopsis/ww/home.html.
23. J. Sambrook, E. F. Fritsch, T. Maniatis, *Molecular Cloning: A Laboratory Manual* (Cold Spring Harbor Laboratory Press, Plainview, NY, 1989).
24. Sequencing templates were prepared by polymerase chain reaction and sequenced with an ABI377 automated sequencer (Perkin-Elmer, Norwalk, CT).
25. Phototropism and hypocotyl growth was assayed as described previously [E. L. Stowe-Evans, R. M. Harper, A. V. Motchoulski, E. Liscum, *Plant Physiol.* **118**, 1265 (1998)].
26. E. Liscum and R. P. Hangarter, *Plant Cell* **3**, 685 (1991).
27. J. W. Reed, P. Nagpal, D. S. Poole, M. Furuya, J. Chory, *Plant Cell* **5**, 147 (1993).
28. C. Bell and J. R. Ecker, *Genomics* **19**, 137 (1994).
29. H.-G. Nam *et al.*, *Plant Cell* **1**, 699 (1989).
30. Information about markers AM40 and AM80 is available at http://www.biosci.missouri.edu/liscum/newmarkers.html.
31. Y. Nakamura *et al.*, *DNA Res.* **4**, 401 (1997); http://www.kazusa.or.jp/arabi/chr5/map/24-26Mb.html.
32. Soluble and total microsomal membrane fractions were separated by ultracentrifugation, followed by two-phase partitioning to enrich for plasma membranes, as described previously [T. W. Short, P. Reymond, W. R. Briggs, *Plant Physiol.* **101**, 647 (1993)].
33. Antibodies against NPH1 were previously described (*7*). Rabbit polyclonal antisera were raised (*22*) against a COOH-terminal NPH3 fusion protein [CBD-NPH3C2 (see Fig. 3A)]. CBD-NPH3 protein was expressed from pET34-Ek/LIC in *Escherichia coli* and purified according to manufacturer's instructions (Novagen, Madison, WI).
34. NPH1-NPH3 interaction was examined in yeast with the Matchmaker Gal4 II System (Clontech, Palo Alto, CA). Expression of fusion peptides was verified by immunoblot analysis (*9*, *22*) with monoclonal antibodies raised against the Gal4 DNA binding domain (GBD) and Gal4 activation domain (GAD) (Clontech).
35. J. H. Miller, *Experiments in Molecular Genetics* (Cold Spring Harbor Laboratory, Plainview, NY, 1972).
36. We thank R. Harper for data in Fig. 1; J. M. Christie and W. R. Briggs for GBD-NPH1 constructs and NPH1 antisera; D. Randall for production of NPH3 antisera; the Arabidopsis Biological Resource Center in Columbus, Ohio, for BAC clones and cDNA libraries; and members of our laboratory for helpful comments on the manuscript. This work was funded by USDA National Research Initiative grant 96-35304-3709, NSF grant MCB-9723124, and University of Missouri Research Board grant RB96-055.

3 June 1999; accepted 17 September 1999

Four Evolutionary Strata on the Human X Chromosome

Bruce T. Lahn* and David C. Page†

Human sex chromosomes evolved from autosomes. Nineteen ancestral autosomal genes persist as differentiated homologs on the X and Y chromosomes. The ages of individual X-Y gene pairs (measured by nucleotide divergence) and the locations of their X members on the X chromosome were found to be highly correlated. Age decreased in stepwise fashion from the distal long arm to the distal short arm in at least four "evolutionary strata." Human sex chromosome evolution was probably punctuated by at least four events, each suppressing X-Y recombination in one stratum, without disturbing gene order on the X chromosome. The first event, which marked the beginnings of X-Y differentiation, occurred about 240 to 320 million years ago, shortly after divergence of the mammalian and avian lineages.

The human X and Y chromosomes, like those of other animals, are thought to have evolved from an ordinary pair of autosomes (*1*). The pseudoautosomal regions at the termini of the X and Y chromosomes still recombine during male meiosis, ensuring X-Y nucleotide sequence identity there. Elsewhere on the X and Y chromosomes, however, X-Y recombination has been suppressed. These nonrecombining regions of the X and Y chromosomes have become highly differentiated during evolution, and only a few X-Y sequence similarities persist within them. These modern X-Y gene pairs are the remaining "fossils" where extensive sequence identity between ancestral X and Y chromosomes once existed. The recent discovery of many X-Y genes has made it possible to examine the entire group to search for patterns of human sex chromosome evolution. Thus far, the human sex chromosomes—the best characterized mammalian sex chromosomes—have been found to contain 19 X-Y gene pairs (*2*).

We first compared the locations of all 19 pairs of genes on the human X and Y chromosomes (Fig. 1). We determined the relative positions of the X-linked genes through radiation hybrid analysis, in many cases confirming previously published localizations (*3*). Map positions of the Y-linked homologs were obtained principally from the literature (*4*–*6*). On the X chromosome, most of the X-Y genes map to the short arm, where they are concentrated toward the distal end. By contrast, the X-Y genes are found as singletons or small clusters throughout the euchromatic portion of the Y chromosome. In general, the map order of the X-linked genes corresponds poorly to that of the Y-linked homologs. Local exceptions to this rule are provided by three small gene clusters that are present on both X and Y chromosomes (Fig. 1).

We next measured, for each of the 19 X-Y gene pairs, synonymous nucleotide divergence between the X-linked and Y-linked coding regions (*7*). Because synonymous substitutions do not alter the encoded protein, they are generally assumed to be nearly neutral with respect to selection. The statistic K_S (the estimated mean number of synonymous substitutions per synonymous site) is often used to gauge evolutionary time (*8*). In the present context, K_S values provide a measure of the evolutionary time that has elapsed since the gene pairs started differentiating into distinct X and Y forms. The calculated K_S values are given in Table 1, where gene pairs are listed according to map order on the X chromosome.

We noted that the 19 K_S values appeared to cluster into approximately four groups (Fig. 2): 0.94 to 1.25 (group 1), 0.52 to 0.58 (group 2), 0.23 to 0.36 (group 3), and 0.05 to 0.12 (group 4). Each X-Y gene pair's K_S value differed significantly from those of all gene pairs in other groups ($P \leq 0.02$). The most striking observation was that, on the X chromosome, the four K_S-defined groups of genes are arranged in an orderly sequence (Fig. 2). X-Y genes are stratified by age along the length of the X chromosome. By contrast, on the Y chromosome, the K_S-defined groups appear to be scrambled (compare Table 1 and Fig. 1).

What might account for the orderly stratification of X-Y genes by age on the human X chromosome? We hypothesize that, during evo-

Howard Hughes Medical Institute, Whitehead Institute, and Department of Biology, Massachusetts Institute of Technology, 9 Cambridge Center, Cambridge, MA 02142, USA.

*Present address: Department of Human Genetics, University of Chicago, 924 East 57th Street, Chicago, IL 60637, USA.

†To whom correspondence should be addressed. E-mail: dcpage@wi.mit.edu

References and Notes

[3] **PKS1, a Substrate Phosphorylated by Phytochrome That Modulates Light Signaling in Arabidopsis**
Christian Fankhauser; Kuo-Chen Yeh; J. Clark Lagarias; Hong Zhang; Tedd D. Elich; Joanne Chory
Science, New Series, Vol. 284, No. 5419. (May 28, 1999), pp. 1539-1541.
Stable URL:
http://links.jstor.org/sici?sici=0036-8075%2819990528%293%3A284%3A5419%3C1539%3APASPBP%3E2.0.CO%3B2-G

[6] **Arabidopsis NPH1: A Protein Kinase with a Putative Redox-Sensing Domain**
Eva Huala; Paul W. Oeller; Emmanuel Liscum; In-Seob Han; Elise Larsen; Winslow R. Briggs
Science, New Series, Vol. 278, No. 5346. (Dec. 19, 1997), pp. 2120-2123.
Stable URL:
http://links.jstor.org/sici?sici=0036-8075%2819971219%293%3A278%3A5346%3C2120%3AANAPKW%3E2.0.CO%3B2-5

[7] **Arabidopsis NPH1: A Flavoprotein with the Properties of a Photoreceptor for Phototropism**
John M. Christie; Philippe Reymond; Gary K. Powell; Paul Bernasconi; Andrei A. Raibekas; Emmanuel Liscum; Winslow R. Briggs
Science, New Series, Vol. 282, No. 5394. (Nov. 27, 1998), pp. 1698-1701.
Stable URL:
http://links.jstor.org/sici?sici=0036-8075%2819981127%293%3A282%3A5394%3C1698%3AANAFWT%3E2.0.CO%3B2-4

LINKED CITATIONS

[7] **LOV (Light, Oxygen, or Voltage) Domains of the Blue-Light Photoreceptor Phototropin (NPH1): Binding Sites for the Chromophore Flavin Mononucleotide**

John M. Christie; Michael Salomon; Kazunari Nozue; Masamitsu Wada; Winslow R. Briggs

Proceedings of the National Academy of Sciences of the United States of America, Vol. 96, No. 15. (Jul. 20, 1999), pp. 8779-8783.

Stable URL:

http://links.jstor.org/sici?sici=0027-8424%2819990720%2996%3A15%3C8779%3AL%28OOVD%3E2.0.CO%3B2-T

[14] **Analysis of the Sequence of Amino Acids Surrounding Sites of Tyrosine Phosphorylation**

Tilo Patschinsky; Tony Hunter; Fred S. Esch; Jonathan A. Cooper; Bartholomew M. Sefton

Proceedings of the National Academy of Sciences of the United States of America, Vol. 79, No. 4, [Part 1: Biological Sciences]. (Feb. 15, 1982), pp. 973-977.

Stable URL:

http://links.jstor.org/sici?sici=0027-8424%2819820215%2979%3A4%3C973%3AAOTSOA%3E2.0.CO%3B2-W

[15] **SMART, a Simple Modular Architecture Research Tool: Identification of Signaling Domains**

Jorg Schultz; Frank Milpetz; Peer Bork; Chris P. Ponting

Proceedings of the National Academy of Sciences of the United States of America, Vol. 95, No. 11. (May 26, 1998), pp. 5857-5864.

Stable URL:

http://links.jstor.org/sici?sici=0027-8424%2819980526%2995%3A11%3C5857%3ASASMAR%3E2.0.CO%3B2-R

[15] **Predicting Coiled Coils from Protein Sequences**

Andrei Lupas; Marc Van Dyke; Jeff Stock

Science, New Series, Vol. 252, No. 5009. (May 24, 1991), pp. 1162-1164.

Stable URL:

http://links.jstor.org/sici?sici=0036-8075%2819910524%293%3A252%3A5009%3C1162%3APCCFPS%3E2.0.CO%3B2-Y

[21] **Signaling Through Scaffold, Anchoring, and Adaptor Proteins**

Tony Pawson; John D. Scott

Science, New Series, Vol. 278, No. 5346. (Dec. 19, 1997), pp. 2075-2080.

Stable URL:

http://links.jstor.org/sici?sici=0036-8075%2819971219%293%3A278%3A5346%3C2075%3ASTSAAA%3E2.0.CO%3B2-G

LINKED CITATIONS

[21] **Routing MAP Kinase Cascades**
Elaine A. Elion
Science, New Series, Vol. 281, No. 5383. (Sep. 11, 1998), pp. 1625-1626.
Stable URL:
http://links.jstor.org/sici?sici=0036-8075%2819980911%293%3A281%3A5383%3C1625%3ARMKC%3E2.0.CO%3B2-U